International Journal of Pharmaceutics 514 (2016) 41–51

Contents lists available at ScienceDirect

International Journal of Pharmaceutics

journal homepage: www.elsevier.com/locate/ijpharm

Combinatorial nanodiamond in pharmaceutical and biomedical applications

Dae Gon Lim[a], Racelly Ena Prim[a], Ki Hyun Kim[a], Eunah Kang[b,*], Kinam Park[c], Seong Hoon Jeong[a,**]

[a] College of Pharmacy, Dongguk University-Seoul, Gyeonggi, Republic of Korea
[b] School of Chemical Engineering and Material Science, Chung-Ang University, 221 Heukseok-Dong, Dongjak-Gu, Seoul, Republic of Korea
[c] Departments of Pharmaceutics and Biomedical Engineering, Purdue University, West Lafayette, IN 47907, United States

ARTICLE INFO

Article history:
Received 8 May 2016
Received in revised form 2 June 2016
Accepted 3 June 2016

Keywords:
Nanodiamond
Drug delivery
Surface
Complex formation

ABSTRACT

One of the newly emerging carbon materials, nanodiamond (ND), has been exploited for use in traditional electric materials and this has extended into biomedical and pharmaceutical applications. Recently, NDs have attained significant interests as a multifunctional and combinational drug delivery system. ND studies have provided insights into granting new potentials with their wide ranging surface chemistry, complex formation with biopolymers, and combination with biomolecules. The studies that have proved ND inertness, biocompatibility, and low toxicity have made NDs much more feasible for use in real *in vivo* applications. This review gives an understanding of NDs in biomedical engineering and pharmaceuticals, focusing on the classified introduction of ND/drug complexes. In addition, the diverse potential applications that can be obtained with chemical modification are presented.

1. Introduction

Nanodiamonds (NDs) have been developed as electric materials since they have promising properties such as energy absorbance, thermal diffusivity, and high capacity (Branson et al., 2013; Lim et al., 2013; Sundar et al., 2014). NDs also have applications in lubricants, composites, electromagnetic shielding, and special catalysts similar to other carbon materials (Mochalin et al., 2012). Recently, NDs have emerged as a new platform for nano/biomaterials due to their interfacial integration with a variety of biomolecules, including proteins, polymers, chemical drugs, and genes. In detail, exploring the biomedical applications of versatile potential ND via chemical modification or physical absorption has been proposed for many different applications including photoacoustic imaging agents, polymer composites as a dental resin (Mochalin et al., 2011), gene carrier (Bertrand et al., 2015; Zhang et al., 2009), drug reservoir (Chen et al., 2009), and fluorescence marker (Schrand et al., 2011). The easy access of NDs to biomedical applications relies on the moderate condition of the surface modifying capability in charges and other functional groups on the ND substrate. Moreover, it has been observed that ND particles uptaken by cells are minimally cytotoxic and biocompatible, which means they do not affect mitochondrial function or ATP production at the cellular level (Schrand et al., 2007a); however, the biocompatibility of ND varies depending on its material properties.

The nature of promising NDs depends mainly on their chemical production and purification procedures. NDs can be produced via detonation method (Mochalin et al., 2012), chemical vapor deposition (Liu and Dandy, 1995), high-energy ion irradiation of graphite (Daulton et al., 2001), and high-energy ball milling of diamond microcrystals (Boudou et al., 2009). Different production methods, treatment conditions, and processing techniques result in diverse types of NDs that vary in size, shape, structure, and even surface chemistry (Kulakova, 2004; Paci et al., 2013; Sabirov and Ōsawa, 2015). This creates distinct surface properties making it possible to use as an extensively good platform for other potential discoveries (Paci et al., 2013). However, this is also why identifying the physical and chemical properties of NDs and carrying out quantitative analysis of its surrounding chemistries remain a challenge (Mochalin et al., 2012).

NDs contain a core diamond crystalline structure and possess a unique surface structure. They have a large specific surface area, high adsorption capacity, and chemical inertness (Kulakova, 2004; Mochalin et al., 2012). Various functional groups in the ND surface

* Corresponding author.
** Corresponding author at: College of Pharmacy, Dongguk University-Seoul, Goyang, Gyeonggi 410-820, Republic of Korea.
E-mail addresses: eakangek@cau.ac.kr (E. Kang), shjeong@dongguk.edu (S.H. Jeong).

http://dx.doi.org/10.1016/j.ijpharm.2016.06.004
0378-5173/

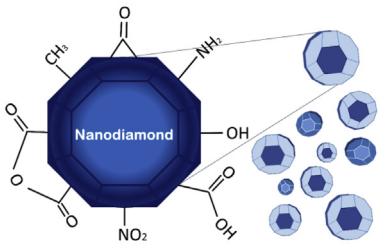

1. Oxygen-containing group
   Hydroxyl
   Carbonyl
   Carboxyl
   Ether
   Anhydride
2. Nitrogen-containing group
   Amine
   Amide
   Cyano
   Nitro
3. Methyl & Methylene
4. Sulfone

Fig. 1. Summary of the functional groups present on the nanodiamond surface.

have been revealed saturation of the reactive surface of carbon atoms (Kulakova, 2004) and existence of dangling bonds for various covalent bonding (Krueger, 2008). These dangling bonds react with the surrounding media to trigger the functionalization of the ND particles (Krueger, 2008).

The ND surface is covered with amorphous carbon and mainly oxygen-containing functional groups [6]. These functional groups are analyzed using Fourier Transform Infrared Spectroscopy (FT-IR), which can detect functional groups and changes in the surface chemistry of functionalized NDs (Chen et al., 2009; Mochalin et al., 2012). Measurements confirm that there is significant presence of oxygen-containing groups on the ND surface (Chen et al., 2009). Small amounts of nitrogen-containing groups, methyl and methylene groups, sulfone, and other groups are also present (Kulakova, 2004). Fig. 1 shows a summary of the functional groups present on the ND surface.

The ND retains amorphous carbon, graphitic shells, and the sp3 phase of carbon on the diamond surface (Gaebel et al., 2012), which is available for surface functionalization. The physicochemical properties of the ND may be altered via surface modification (Sabirov and Ōsawa, 2015). Functional groups can be replaced by other groups, but they always remain attached within the surface of the ND (Kulakova, 2004). They can also be the binding site for the covalent integration of ND into polymer structures and help improve the dispersibility of ND powders in common solvents (Liu et al., 2004). Various groups are compatible with ND surface chemistries, allowing for radical surface functionalization, and thus present a distinct characteristic of ND compared to other nanoparticles (Mochalin et al., 2012; Wahab et al., 2015); ND also exhibits high surface reactivity compared to other carbon nanostructures. ND is chemically functionalized in many ways, but the outcome depends on the purity and uniformity of their surface chemistry (Fig. 2) (Mochalin et al., 2012; Sabirov and Ōsawa, 2015; Wahab et al., 2015). Surface functionalization was also said to affect the stability of ND surfaces (Mochalin et al., 2012). The functionality of the ND surface is responsible for its drug binding ability and imaging, and is also a determining factor for its other applications (Paci et al., 2013).

With these specific potentials and capabilities, ND complexes that are formed either by physical adsorption or chemical conjugation have the benefits of reducing the multidrug resistance of anticancer drugs, enhancing delivery efficacy with convective diffusion. This property of ND complexes may possibly be useful for diverse smart designs (Wang et al., 2014). Small ND of 5 nm diameter can perform as a carrier platform by holding drug molecules within an intracellular compartment due to their large surface area. Moreover, ambiguous surface functional groups and their density on the ND have dependence on versatile sources. This review summarized the versatile chemical modifications of NDs required to develop its desirable properties, the potentials of ND as a drug delivery carrier platform, and the fate of ND within cells and other *in vivo* applications. Future applications of ND were also discussed with the objective of creating pharmaceutical applications.

2. Molecular dynamics

Possible concepts of versatile and novel ND applications have been disclosed in several recent studies, which have made a strong driving force towards analogous goals. However, different commercial sources of NDs provide ambiguous and veiled surface characteristics that require fundamental understanding and methodology standardization in ND experiments (Lai and Barnard, 2014). Understanding the faceted ND surface is a critical step in taking advantage of the high surface area to volume ratio for biomedical and pharmaceutical applications. Furthermore,

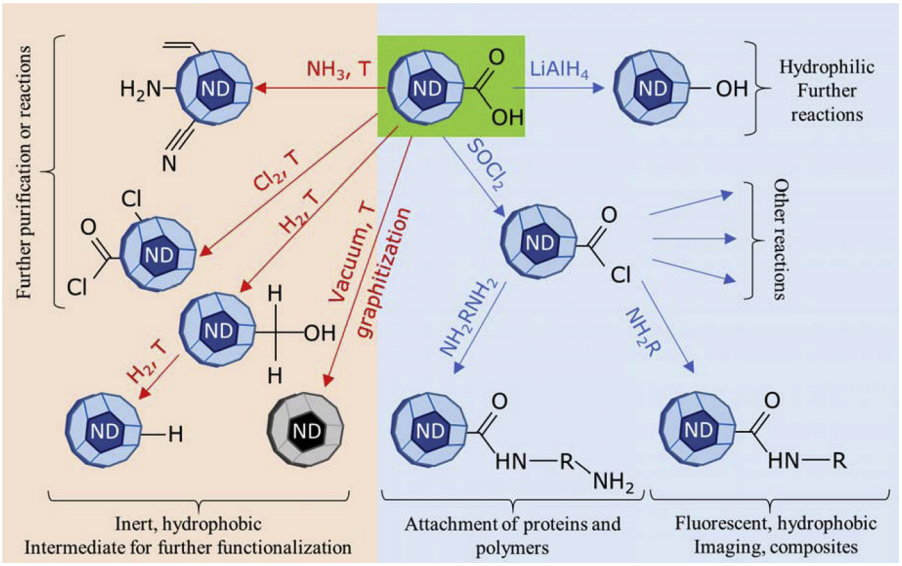

Fig. 2. Schematic description of ND surface modification. Carboxylated ND (ND–COOH) is a common starting material. The surface of ND–COOH can be modified by reaction with gas at high-temperature condition (red area) or wet chemistry modification at ambient-temperature condition (blue area). (Adapted by permission from Mochalin et al., Copyright 2012 Macmillan Publishers Ltd.). (For interpretation of the references to colour in this figure legend, the reader is referred to the web version of this article.)

stoichiometric adsorption of biomolecules on ND surface needs to be clarified based on the understanding of its properties.

Regarding this aspect, several computer simulations and molecular dynamics have given fundamental insights into bare NDs. The adsorption strength of bare NDs was investigated with regard to the distribution of basic functional groups such as COOH, OH, O, and H at the atomic level (Lai and Barnard, 2014). It is said that the surface reconstruction by functional groups specifies facet orientation and that ultimate particle shape determines the concentrated adsorbents on ND surfaces. Facet (111) provides the crowded density of COOH groups, resulting in weak adsorption. It is interesting that the size and shape of facets are also one of the factors for determining the surface properties of NDs, resulting in its varied adsorption ability. Barnard et al. extensively studied the effects of shape and size on NDs (Barnard and Per, 2014; Barnard and Sternberg, 2005). The electro-potentials of the surface become different depending on the shape, which might be a critical factor in determining the ND properties in an aqueous solution. The degree of protonation in the edges and corners of ND facets may vary depending on the size of the facets.

ND itself is influenced by the factors of its exterior environment such as the temperature and pH (Adnan et al., 2011; Lai and Barnard, 2012). Together with the basic understanding of ND such as its molecular dynamics, the behavior of ND complexes with drugs has also been investigated. One study simulated the pH dependent interaction between doxorubicin (Dox) hydrochloride and faceted ND (Guan et al., 2010). Molecular dynamics suggests that the manner in which Dox adsorption on ND depends on the pH. In ND/Dox complexes, ND was integrated with 30% functional groups at different pH levels. As shown in Fig. 3, it was noted that Dox was located at 15 Å from the ND surface at low pH, maintaining a stable separation. Dox was bound to the ND surface at high pH, indicating that the electrostatic interaction was strong enough (Adnan et al., 2011). The pH dependent behavior of ND might change depending on the major surface functionality. In addition to pH adjustment, van der Waals forces, hydrogen bonding, and facet-dependent dipole moments are also factors in determining ND aggregation and drug adsorption. It is critical to understand completely how the relationships between diverse factors influence ND agglomeration and drug adsorption.

In an advanced study, a multiscale simulation of siRNA gene delivery was carried out with polyethyleneimine (PEI)-based ND complexes (Kim et al., 2012). From the first layer of PEI on ND, the simulation estimated the number of PEI to the ND and the effective ratio of siRNA adhering to the PEI/ND surface. It was noted that the approach of the large molecule, PEI, was limited depending on the facet size and facet direction.

3. Nanodiamond in biomedical imaging

3.1. Fluorescence nanodiamond with nitrogen-vacancy sites

Laser-irradiated ND with nitrogen-vacancy color center is known to possess fluorescence and magnetism characteristics, which make it useful for smart applications in nano-scaled biolabeling and bioimaging (Faklaris et al., 2009; Havlik et al.,

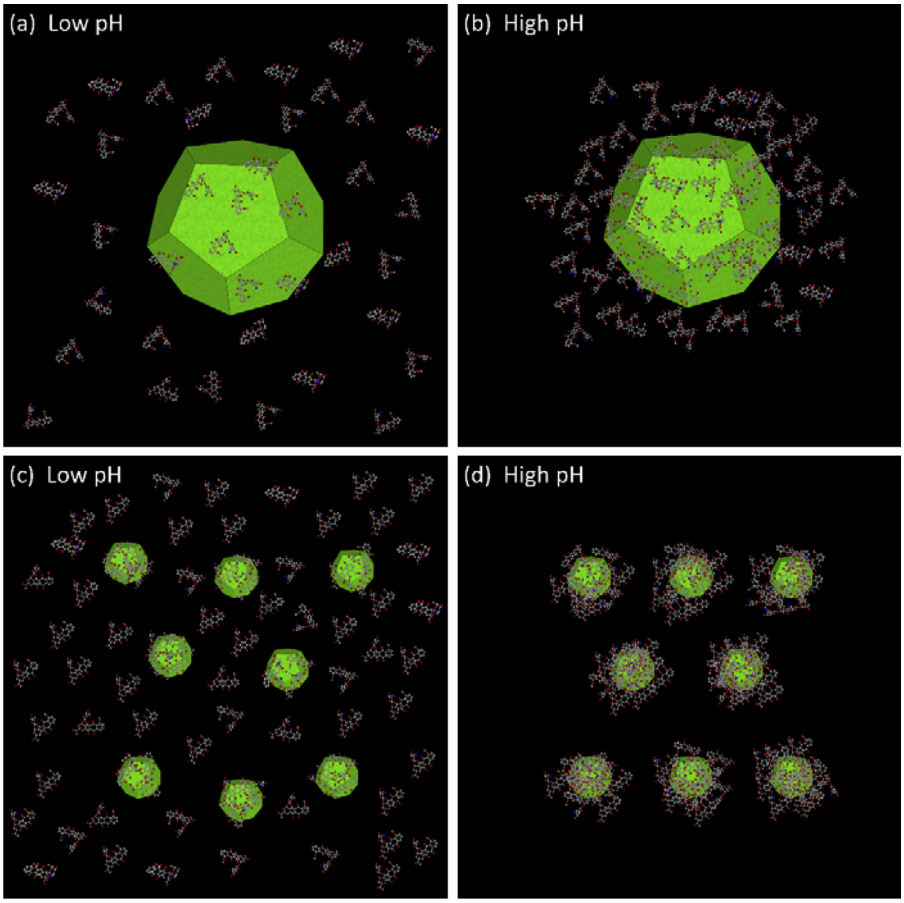

Fig. 3. pH-dependent doxorubicin (Dox) adsorption on the ND surface. Magnified ND–Dox complex at (a) low pH and (b) high pH. The electrostatic interactions of ND with Dox are close to minimum at low pH, while their strong electrostatic interactions lead the Dox molecules to be adsorbed on the ND surface at high pH. Schematic view of modeling with eight NDs at (c) low pH and (d) high pH (modified with permission from Adnan et al., Copyright 2011 American Chemical Society).

2013). Since the first direct observation of 5 nm fluorescence diamond (FND) was made, ND has garnered growing interests as a promising material (Bradac et al., 2010; Wrachtrup, 2010). The long-lasting optical properties of laser-irradiated ND with nitrogen vacancy sites were enhanced with the addition of a silica shell coating (Prabhakar et al., 2013). This nanocomposite material with ND provided continuous cellular tracking due to its stable photoluminescence. The PEG-PEI-coated ND provided improved cellular uptake, showing localized FND at subcellular regions (Prabhakar et al., 2013). Moreover, the long term stability and biocompatibility of laser-irradiated fluorescence ND *in vivo* was examined. The development of the intrinsic properties of FND was also investigated with photostability, imaging resolution, and fluorescence intensity (Vaijayanthimala et al., 2012). However, FND with a nitrogen-vacancy color center is not widely used due to its price and limited production. The FND production method varies depending on the ND source, input energy, and ion species (Nagl et al., 2015). The accurate set-up of FND production and the biomedical applications of FND still have a lot of areas to be examined.

3.2. Fluorescence diamond with extrinsic dyes

Fluorescence dyes as a model drug were complexed with ND via physical adsorption (Chang et al., 2008; Lien et al., 2012). The studies provide insights about novel ND nanocomposites as a tool for bioimaging and drug delivery platforms. Since it is not easy to access ND with nitrogen vacancy sites due to the high cost of the equipment and unfamiliarity with the methods of production, alternative approaches to introduce extrinsic fluorescence dyes have been achieved via conjugation onto the ND surface (Hens et al., 2008; Schrand et al., 2011). Coupled ND complexes between aminated ND and reactive *N*-hydroxysuccinimide (NHS) functionalized TAMRA were utilized for temporal and mechanistic cell tracking (Schrand et al., 2011). Co-localizations, early endosomes, or lysosomes in N2A cells were traced over time. The destination of ND localization into respective cell compartments may enhance the targeted site-specific drug delivery of genes or proteins. TAMRA conjugated with ND plays a role as a bright biomarker with high fluorescence intensity, probably due to the high reactive sites of ND.

3.3. Blue fluorescence nanodiamond

Blue fluorescence ND formed via wet chemistry has potential in ND surface modification with small molecules to change the light absorption characteristics and to emit diverse light energy states (Mochalin and Gogotsi, 2009). The formation of fluorescence ND via the wet chemistry method is promising and elaborate studies are still required to understand the complete mechanism. Blue fluorescence ND was obtained by the conjugation of octadecylamine (ODA), which was excited at 410 nm and emitted at 450 nm. Another study noted that the conjugation of oligo(phenylenevinylene) onto the ND surface showed enhanced photoluminescence as the agglutinate size of ND increased with the ND concentration as shown in Fig. 4 (Maitra et al., 2011). From the comparison of ODA modification, the photoluminescence of oligo(phenylenevinylene)-conjugated ND was stronger than that of ODA-conjugated ND, indicating that the molecular design at the ND surface could be a critical factor for fluorescence. The close distances between ND agglutinates performed as bridges for electrons hopping between particles. Oligo(phenylenevinylene) moiety on the ND surface helps ND store electrons and transfer energy. ODA or oligo (phenylenevinylene) conjugated ND with blue fluorescence are hydrophobic. Hydrophilic ND with fluorescence is issued for use in widespread biomedical imaging.

4. The cellular response, biocompatibility, and biodistribution of nanodiamond

Varieties of nanoparticles have been introduced into the body to examine their biocompatibility and biodistribution. The fate of nanoparticles in the body has been traced both *in vitro* and *in vivo*. The surface properties of nanoparticles can reduce enzymatic degradation or phagocytic attack, extending ND circulation *in vivo* (Vaijayanthimala et al., 2012). Since ND has been used as a new material in biomedical applications, continuous studies have been performed that have proved that ND is inert, biocompatible, and less toxic than many alternatives. Opening with new ND biomedical and pharmaceutical applications, extensive and quantitative studies are still necessary to examine cellular response, biocompatibility, and biodistribution. Moore et al. investigated the cellular response of detonated ND, fluorescence ND, and amine ND in HeLa and HepG2 cell lines (Moore et al.,

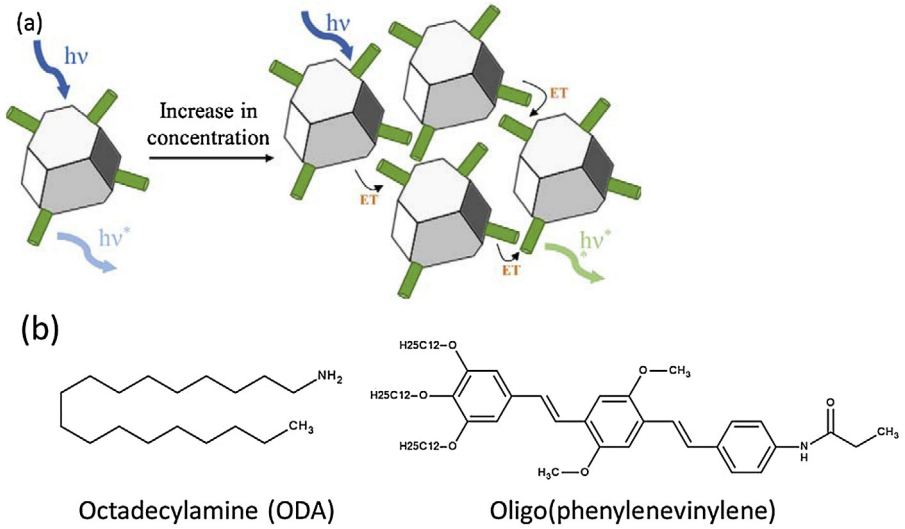

Fig. 4. The schematic features of ND energy absorbance and transfer to neighboring ND complexes. (a) ND agglutinates performing as bridges for electron hopping and (b) the chemical structure of ODA and oligo(phenylenevinylene). (Reproduced from Maitra et al., Copyright 2011, with the permission of The Royal Society of Chemistry).

2014). ND at 25 μg/mL concentration did not show promoted apoptosis, an inflammatory response, or inhibited proliferation at the level of the transcriptional response. Moreover, ND/daunorubicin complexes at a ratio of 5:1 showed less toxicity at an equivalent dose of the free drug for metabolic activity, cell death from lactate dehydrogenase release, and initial apoptosis from caspase activity (Man et al., 2014). Simple physical drug adsorption onto the ND and subsequent cellular treatment *in vitro* showed potentially promising results as a new drug reservoir. However, it should be noted that the stability of the ND complexes was not examined over time in biological media and with appropriate exposure to ND or ND/drug complexes into cells.

Several studies have shown that bare ND is less toxic compared to other carbon materials such as carbon nanotubes, graphenes, and graphites (Paget et al., 2014; Schrand et al., 2007b; Zhu et al., 2012). Fluorescent dye-conjugated ND was injected to mice for biodistribution study. ND was accumulated in the lung, liver, spleen, and kidney in a day and its clearance lasted over 10 days. Moreover, fluorescence signal was also observed in the bladder (Chow et al., 2011). When ND, graphite, and graphene oxide nanoparticles were injected to rats intraperitoneally, ND showed significantly less aggregates in mesentery, connective, and abdominal lipid tissue compared to graphite and graphene oxide nanoparticles (Kurantowicz et al., 2015). The biocompatibility and biodistribution of ND still have critical issues for further realistic applications. Inert bare ND and heparin/polyarginine-coated ND showed dramatically improved hemocompatibility compared to the group of graphene (Li et al., 2013). Liu et al. observed the cellular tracking of fluorescence-labeled ND in an A549 cell (Liu et al., 2009). It was noted that ND agglutinates were localized in the interphase and mitotic phase (prophase, metaphase, and telophase). ND was also separated and localized into two daughter cells. ND was shown in all cell cycle phases, while not disturbing the spindle formation or chromosome segregation. The study proved that endocytic ND agglutinates were not cytotoxic in cell division and differentiation over 10 days of long term observation. One study by Marcon et al. also examined the cytotoxicity of NDs with different surface functionalities (–OH, $–NH_2$, –COOH) in HEK293 cells and Xenopus laevis embryos (Marcon et al., 2010). No cytotoxicity was present in up to 50 μg/mL of ND in HEK293 cells, while the embryotoxicity for carboxylated ND was shown for both gastrulation and neurulation. Moreover, Rojas et al. studied *in vivo* ND biodistribution using radioactive ^{18}F-labeled ND (Fig. 5) (Rojas et al., 2011). The individual particle sizes of surface modified ND was approximately 7 nm, while aggregates in aqueous solution were approximately 680 nm, as measured by light scattering that required surfactants in their dispersion solvent of up to 5% (Rojas et al., 2011). Interestingly, prefiltered NDs showed a highly excreted distribution into the urinary tract, proving that stable NDs aggregates in size are critical for biodistribution and excretion. The long term toxicity study of ND in rats was also investigated (Vaijayanthimala et al., 2012). Fluorescence ND was administered with subcutaneous, intradermal, and intraperitoneal injections for a dose per week, and rats were sacrificed for the tissue morphology after 12 weeks. Dark carbon-laden cells were observed in the dermis with no tissue damage, inflammation, or necrosis in the

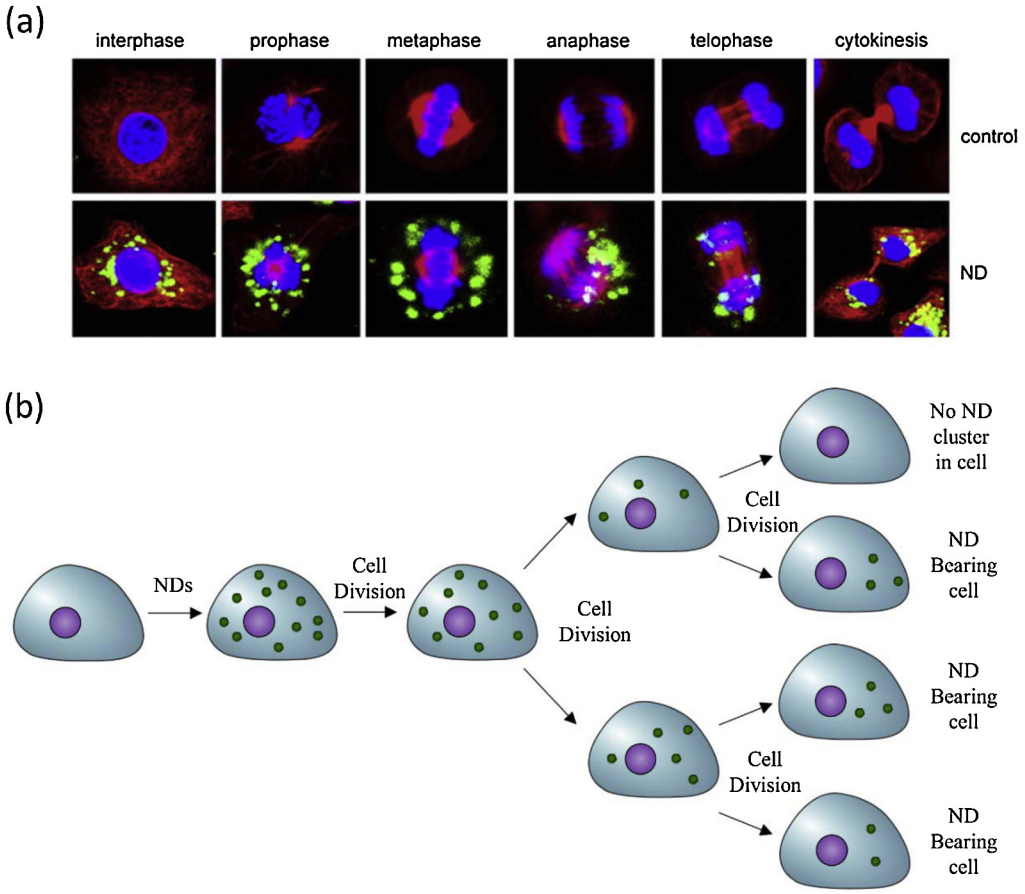

Fig. 5. Cellular trafficking of ND agglutinates in cell cycles and division. (a) The tracking of ND agglutinate at each cellular phase. ND agglutinates were localized in the interphase and mitotic phase (prophase, metaphase, and telophase), (b) Schematic picture of the suggested mechanism of ND localization. (Reproduced from Liu et al., Copyright 2009, with permission from Elsevier).

surrounding cells. Promising results of ND applications *in vivo* have been shown in a way, yet further extensive studies should be performed for broader and more realistic ND applications.

5. Nanodiamond dispersion

Unusually strong aggregates of ND lead to elaborating the deagglomeration steps of grinding, milling with salts (Pentecost et al., 2010), sonication with the addition of salt, and the addition of surfactant (Xu and Zhao, 2012; Xu et al., 2005). Without impairing the intrinsic properties of NDs, the efforts to prepare well-dispersed NDs in an aqueous solution have been performed. Detonated ND is approximately 5 nm in size, but often forms named aggregates or agglutinates in the range of several hundred nanometers in aqueous solution (Chang et al., 2011). At present, ND can be classified according to its agglutinins and disintegrated aggregates. Agglutinin ND is bound with covalent C—C bonds between internanocrystals, forming unusually strong tight aggregates. Even under strong ultrasonication, agglutinates are stable without disintegration. Disintegrated NDs are composed of agglutinate and small aggregates interconnected by van der Waals forces and electrostatic interaction. NDs have been heavily functionalized with hydrophilic groups on its surface including phenylated, carboxylated, and sulfonylated NDs to produce water-dispersible NDs. These functional groups help in the production of a stable dispersion of NDs in aqueous solution ($\leq$100 μg/mL) via mild ultrasonification (Huang et al., 2007). It was hypothesized and confirmed that the carboxyl group on the ND helped the ND interface ND/drug complexes through physiosorption and electrostatic interactions (Chen et al., 2009). The dependence of the ND functional group on ND/drug complexes has been characterized with ND/drug imaging and UV–vis analysis, and various ND surface modifications grant specific functionalities. However, ND aggregation (cluster formation) in biological solutions limits its wider applications.

One simulation suggests that a ND with a hydroxyl group is more thermodynamically stable than a ND with a carboxyl or an amine group (Krueger and Lang, 2012), and the size of agglutinates is greatly dependent on Coulombs law by the van der Waals interaction rather than electrostatic interaction (Chang et al., 2011). It was reported that a varied facet size originates the dipole moments, determining the final size of the ND agglutinates (Lai and Barnard, 2014). It was also reported that ND aggregates can cause DNA damage in embryonic stem cells (Xing et al., 2011); the results implied that the cellular damage caused by the ND was probably due to the unacceptable agglutinate size in the intracellular compartment. Thus, for ND to be exploited in biomedical and pharmaceutical areas as a drug delivery platform, the stable dispersion of ND in aqueous and biological solution is critical. Surface modified ND with high purity also showed a narrow distribution in an aqueous solution (Kuznetsov et al., 2012). Ultimately, chemical surface modification may be required to disperse the NDs evenly in aqueous solution and be further circulated when *in vivo*.

Niu et al. showed promising potentials, proving that the photoluminescence of the ND itself could be controlled by laser chemistry (Niu et al., 2011). Laser irradiation on the ND resulted in the ablation of the amorphous carbon layer and a disconnection between ND agglutinates. Unusually strong ND agglutinates could be controlled by laser irradiation with the addition of a PEG surfactant. The ND size distribution was critically varied, resulting in unique light absorption and photoluminescence. The study showed the relevant importance of ND surface modification and dispersion.

6. Nanodiamond drug delivery

6.1. Physical adsorption of small molecular drugs

The most important advantages of ND as a drug delivery platform arise from its strong physical adsorption. The intrinsic properties of ND adsorption originated from its high surface area to volume ratio and its facet-dependent dipole moment. Even the organic impurities were absorbed within the ND, or the ND contained bound and even absorbed water at its molecular level. The absorbed water is not easily removed, even during drying procedures (at 393 K), because it is absorbed inside the ND pores that form upon aggregation (Kulakova, 2004). The strong capability of physical absorption is known to be controlled by the ND surface functional groups that can also be modified via oxidation such as through simple acid-washing (Krueger and Lang, 2012).

The chemical conjugation of prodrug onto the ND surface by microwave-assisted paclitaxel conjugation has been suggested to facilitate the functionality of the ND surface and increase the drug loading efficiency; the chemical conjugation of paclitaxel doubled the loading efficiency (Hsieh et al., 2015). It was also reported that polyglycerol was conjugated on the ND surface as a linker (Zhao et al., 2014a). Arg-Gly-Asp (RGD) cell penetrating peptide sequence and Dox were conjugated at the end of the polyglycerol. ND–polyglycerol with Dox in the respective cell line showed selective effects with minimal uptake and toxicity in a macrophage, while being highly sensitive to the drug in cancer cells.

In fact, rather than the chemical conjugation of prodrug, ND/drug delivery via physical adsorption was intensively reflected in diverse studies due to its simple process. Oxidized and bare ND has often been investigated for its sorption of heavy metal, dyes, proteins, and chemical drugs (Chernysheva et al., 2015; Chu et al., 2014; Manus et al., 2009; Wang et al., 2012). To understand the ND fundamentals as a drug delivery carrier, Mochalin et al. studied ND agglomeration/deagglomeration and the adsorption capacity of different drugs (Mochalin et al., 2013). The surface functional group on ND with amine, carboxyl, and hydrogen groups showed varied adsorption levels for Dox and polymyxin B. ND dispersion and the drug solution being dependent on the pH condition require clarification, since the solubility of Dox is also changed, according to pH. The ionized and charged surface functional groups on NDs at adapted pHs also alter the drug adsorption capacity. Salaam et al. studied the ND–Dox complexes formed by physical adsorption (Salaam et al., 2014a; Salaam et al., 2014b). The release of those complexes was investigated as the pH changed. Since Dox was solubilized at low pH, accelerated Dox release was expected at low pH. It is not evident that pH controlled release is mainly attributable to the ND surface reservoir ability or the intrinsic properties of Dox. The promising desorption control of a drug, which is an important property of therapeutics, is shown in this study. Rye et al. also developed ND/Dox complexes, particularly using microfluidic devices (Ryu et al., 2015). The simple process of microfluidics controlled the size of the ND/Dox agglutinate, which facilitated cellular uptake. Approximately 50 nm of the ND agglutinate was shown to have high cellular uptake. Moreover, ND/Dox complexes were investigated for their ability to inhibit the lung metastasis of breast cancer (Xiao et al., 2013). Drug loading was carried out with a 5:1 weight ratio of ND to Dox. To prolong the *in vivo* circulation, 5% PEGylated positively charged amine lipid molecules were also used to coat the ND/drug dispersion. Though the ND/Dox lipid vesicles showed low cytotoxicity and therapeutic potential, it was ambiguous whether the enhanced anti-metastatic effect resulted from the ND/drug complexes or the aid of lipid vesicle formulation.

The study to investigate *in vivo* biodistribution also showed that 1,2-distearoyl-sn-*glycero*-3-phosphoethanolamine (DSPE)-PEG lipid–coated NDs and poorly water soluble sorafenib complexes enhanced the circulation time *in vivo* (Zhang et al., 2014). The residual drug concentration in tissue was improved 15-fold, compared to bare ND/sorafenib complexes without lipid coating, and inhibited tumor growth in tumor xenograft models. ND used for the physical adsorption of mitoxantrone possessed highly positive zeta potential and probably hydrogenated ND (Toh et al., 2014). Mitoxantrone adsorption resulted in a slight decrease of positive zeta potential. It can be suggested that the π–π interaction and hydrogen bonding with the ND surface are major interacting forces with mitoxantrone, imposed from the structure of mitoxantrone. The release of mitoxantrone was accelerated at low pH, indicating that the physical adsorption of the drug on NDs has potential for use in controlling the manner of drug release.

Anticancer drug delivery with specific targeting has been examined, mainly focusing on overcoming multi-drug resistance (MDR) with cancer cells. Surprisingly, ND showed increased anticancer drug retention and thus antitumor activity. ND complexes with Dox showed increased acute apoptotic responses and enhanced drug retention compared to treatment with Dox alone in MDCK-MDR drug resistant cells (Chow et al., 2011). ND-enhanced delivery and decreased drug efflux was not only defined for solid tumors but also effective in leukemia cancer cells. ND–daunorubicin (DNR) complex showed lower IC_{50} values and efficacy against drug resistant K562 leukemia cells (Man et al., 2014). The pH dependent release of drugs was exampled using DNR in leukemia that was bound via simple physical adsorption (Man et al., 2014). pH-dependent ND/DNR complexes showed significantly reduced gene expression of three major efflux proteins in the ATP-binding cassette (ABC) transporter. ND/DNR complexes were hypothesized in which NDs played a role as stable drug-releasing platform and bypassed the efflux pump, elevating the drug concentration within cells and thus enhancing the drug's therapeutic efficacy. It was suggested that the ND/drug delivery platform assisted the reduction of multidrug resistance in cancer cell lines. Active drug efflux transporters such as ABC transporters cause anticancer drug resistance against anthracyclines such as Dox and DNR (Schinkel and Jonker, 2003). Drug conjugates with NDs might evade drug efflux transporters by entering the cell through endocytosis (Zeng et al., 2014). The therapeutic effect of epirubicin-adsorbed ND was investigated against chemoresistant hepatic cancer *in vivo* (Fig. 6) (Wang et al., 2014). The epirubicin–ND complex also showed improved antitumor activity and reduced multi-drug resistance effects when compared to epirubicin alone and an ND-treated group. The complex formation between epirubicin and ND prevents the efflux of epirubicin via ABC transporters due to the change of molecular size and structure (Wang et al., 2014).

Enhanced convective drug delivery associated with the drug and NDs prevents drug efflux via the ABC transporter. The extended drug retention within cells elevates the possibility to target passively in the intracellular compartment, and thus facilitates the inhibition of initial cancer stem cells mediated with tumor growth. NDs not only reduce drug resistance but also prevent the side effects associated with a high drug concentration. Dox showed myelosuppression, systemic immune response, and liver toxicity at a high concentration. ND/drug complexes might be an alternative delivery platform, replacing the small molecules of an ABC transporter inhibitor. Though ND/drug complexes provided high loading efficiency as a capable drug reservoir, specific formulations seemed to be demanded for ultimately long lasting *in vivo* circulation and targeting. Surely, developing the method of ND use in optimal pharmaceutical formulations is required in the near future to approach realistic therapeutic agents. Table 1 lists various examples of nanodiamond/drug complexes.

6.2. Adsorption of biomolecules onto nanodiamonds

Together with the adsorption of small molecular drugs, the adsorption of relatively large biomolecules onto the ND surface has become an emerging interest as a new therapeutic delivery platform. A fundamental understanding of ND/biomolecule (proteins, siRNA, and DNA) complexes grants insight into the biomolecular array on NDs. The protein size, surface charge, and complex ratio of protein to NDs are the determining factors that form the biomolecule layer on the ND.

Protein adsorption was examined with different surface charge functionalities on NDs (Aramesh et al., 2015). The small protein lysozyme formed multilayers with significant conformational changes, while the large protein albumin formed monolayers with minimal conformational changes on the ND surfaces. Depending on the surface charges on ND, the protein conformation and array between proteins become distinct. One particular study investigated the quantitative analysis of ND/protein adsorption by ratio (Lin et al., 2015). A ND with 3.7 nm in diameter possessed a saturated surface forming 1:1 myoglobin/ND complexes of the protein myoglobin with a molecular weight of 17 kDa. Another study reported that the physical adsorption and desorption of insulin onto NDs could be controlled in modulated pH environment (Shimkunas et al., 2009). Insulin was desorbed from the ND

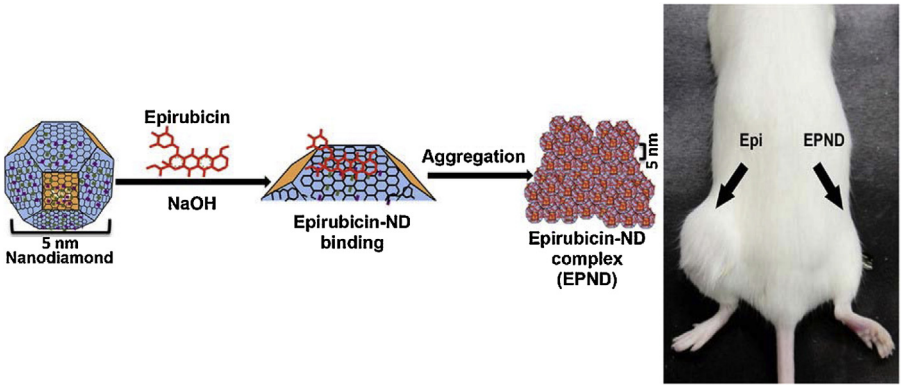

Fig. 6. Schematic description of epirubicin–ND complex formation and the tumor-initiation evaluation of epirubicin–ND complex. Epirubicin-ND complex prevented secondary allograft tumor formation compared to only epirubicin treated case at enhanced tumor-initiation evaluation in allografts when seeded at 300 tumor cells per injection (Reprinted with permission from Wang et al., Copyright 2014 American Chemical Society).

Table 1
The physical properties of nanodiamond/drug complexes.

Mechanism	ND-Source	Drug	Diameter (nm)	Surface charge (mV)	Ref.
Covalent linkage	ND-COOH	Recombinant growth hormone	9.3	N.D.	Chu et al. (2014)
	ND-COOH	a2b1 integrin-binding peptide	303	17	Knapinska et al. (2015)
	ND-PEG	Cisplatin	66.9	N.D.	Zhao et al. (2014b)
	Pristine ND	Paclitaxel	10	N.D.	Liu et al. (2010)
Physical adsorption	ND-COOH	Purvalanol A	556	27.2	Chen et al. (2009)
	ND-COOH	Hydroxytamoxifen	278.9	25.7	Chen et al. (2009)
	ND-COOH	Dexamethasone	77.55	21.9	Chen et al. (2009)
	ND-COOH	Transferrin/doxorubicin	235	N.D.	Wang et al. (2015)
	ND-COOH	Daunorubicin	93.1	N.D.	Man et al. (2014)
	ND-DGEA	Doxorubicin	89	21	Salaam et al. (2014a)
	ND-Gd	Epirubicin	89.2	19.6	Wang et al. (2014)
	ND-H	siRNA	30	−15	Bertrand et al. (2015)
	ND-NH2	Plasmid DNA (GFP)	100	35	Zhang et al. (2009)
	ND-PEG	Doxorubicin	187.7	−27.8	Wang et al. (2013)
	ND-PEI600	Plasmid DNA (GFP)	250	45	Zhang et al. (2009)
	Pristine ND	Bovine Insulin	1690	−12	Shimkunas et al. (2009)
	Pristine ND	Myramistin	150	29	Chernysheva et al. (2015)
	Pristine ND	Sorafenib tosylate/DSPE-PEG	127.6	N.D.	Zhang et al. (2014)
	Pristine ND	Mitoxantrone	54.6	47.8	Toh et al. (2014)
	Pristine ND	Bone morphogenetic proteins	120	N.D.	Moore et al. (2013)
	Pristine ND	Alginate/Cisplatin	486.9	−14.8	Cui et al. (2016)
	Pristine ND	Amoxicilin	143.1	46.08	Lee et al. (2015)

and released into the cell at high pH. However, it should be noted that the hydrodynamic diameters of NDs and insulin/ND complexes range over 1 μm; a simple pH adjustment might modulate the exterior charge of the protein and the ND aggregation. Protein stability and dispersion stability need to be clarified at each pH, forming stable ND complexes with stable colloidal properties.

siRNA, which is smaller than proteins, might be more applicable in ND complexation. Hydrogenated ND with a highly cationic positive charge (50 mV of zeta potential) have been effective at binding therapeutic siRNA (Alhaddad et al., 2011), which was successfully targeted against the Ewing sarcoma junction and oncogenes, strongly inhibiting its expression in cells. The cellular tracking of ND supported that ND in dense aggregate forms were localized in multivesicular cell bodies and proteins in late endosomes. Due to strong cationic charges, hydrogenated ND was an effective siRNA delivery platform. In the case of oxidized NDs with negative charges, ND with cationic polymers such as PEI and polyallyamine were layered for the vectorization of siRNA (Alhaddad et al., 2011). They suggested that cationic polymeric layers on NDs can modulate the internalization pathways. PAH-coated ND/siRNA complexes promoted internalization through predominant clathrin-mediated endocytosis, while PEI-coated ND/siRNA facilitated clathrin-mediated endocytosis and macropynocytosis.

Charged peptide biomolecules were directly delivered on ND surface. Protamine, a biodegradable and positively charged peptide polymer, adsorbed onto the NDs through hydrogen bonding or electrostatic interaction (Cao et al., 2013). Protamine is mainly composed of positive arginine peptides, which are known to restore downregulated MiR-203 in tumors such as esophageal, gastric, and colorectal cancers. The restoration of MiR-203 expression by the delivery of micro-RNA ND/protamine complexes inhibits tumor cell proliferation, migration, and invasion. It is noted that micro-RNA/ND/protamine complexes are also successfully vectorized in the intracellular compartment, showing that a ND is effective as a gene vector for using large molecules as delivery platforms and therapeutics. Highly dense positive charges on the ND surface provided stable micro-RNA residence during vectorization into the cellular compartment.

6.3. Complexes with biopolymers

The diverse chemical modifications of the ND surface are easily accessed due to the abundant surface modality. The chemical end groups on the ND surfaces have been conjugated with extended functional chemical designs including dopamine derivatives (Barras et al., 2011), versatile biopolymers (Barras et al., 2011; Lee et al., 2013), functional groups including biotin (Krueger et al., 2008), and fluorescence in small molecules (Hens et al., 2008).

Together with abundant chemically modulated ND surfaces, biopolymers with reactive groups have been combined with ND, augmenting intense layering. One particular study investigated NDs encapsulated in a PEI/chitosan nanogel (Kim et al., 2014). The ND-embedded PEI/chitosan nanogel provided a sustained release of timolol from the hydrogel lens, as lysozyme activates the enzymatic degradation of chitosan. The loading of ND-embedded PEI/chitosan nanogel into a poly (2-hydroxyethyl methacrylate) (polyHEMA) lens also improved the mechanical properties of Young's modulus and the tensile strength. ND conjugated with thermosensitive poly(*N*-isopropylacrylamide) (polyNIPAM)/dopamine derivatives preserved the properties of thermosensitive polyNIPAM and presented the reversible temperature-dependent aggregation of ND complexes, which probably resulted from the hydrophobic/hydrophilic alignments of polyNIPAM (Barras et al., 2011).

Poly(ethylene glycol)-*b*-poly(2-(dimethylamino)ethyl methacrylate-co-butyl methacrylate) (PEG-b-P(DMAEMA-co-BMA)) was used for non-covalent coating on the ND (Lee et al., 2013). The block copolymer was composed of positive charged moieties to attract negatively charged carboxylic moieties on the ND. At the same time, hydrophobic moieties could interact with the hydrophobic ND surface (Lee et al., 2013). Moreover, the PEG block formed hydrophilic shell to prevent the aggregation of ND. The study suggested that the stable dispersion of the ND might be compromised by the interactions between hydrophobic forces, electrostatic interaction, and the repelling force of the polymer. It was noted that the design of the polymer and the colloidal properties of ND made it critical for stable dispersions. Surface-modified NDs that are compatible in an aqueous solution will surely provide a platform for many biomedical applications.

ND was also embedded in biopolymeric matrixes with a stimulating protein to induce tissue regeneration. There have been significant efforts to develop a biocompatible substrate that can support biomimetic matrices and perform a controlled release of drugs (Huang et al., 2008; Mansoorianfar et al., 2013; Xing et al., 2013). ND was incorporated into the structure of the natural extracellular matrix (ECM), and promoted the adsorption of cell adhesion–mediating molecules in an advantageous geometrical conformation (Bacakova et al., 2014). In addition, ND has been shown to increase the surface area of scaffolds, allowing for numerous non-covalent interactions between the scaffold surface and proteins (Tsapikouni and Missirlis, 2008). For example, the ND surface was functionalized with bone morphogenetic protein-2 (BMP-2), to induce localized bone regeneration (Kloss et al., 2008). BMP-2 adsorbed onto ND/poly(ι-lactide)-co-(ε-caprolactone) copolymer scaffolds promoted *de novo* bone formation in *in vitro* human mesenchymal stem cells and *in vivo* mandibular defected rats, demonstrating the potential of integrating ND into tissue-engineering disease applications (Suliman et al., 2015).

7. Pharmaceutical concerns and remarks

The biomedical applications of carbon materials including carbon nanotubes, graphite, graphite platelets, and graphene nanosheets and dots have been widely used as multifunctional carriers. The recently developed material, nanodiamond, is garnering increasing interest as a multifunctional drug delivery platform. The ND has been proven to possess low toxicity in cells, and high *in vivo* biocompatibility and biodistribution. In addition, the UV protection (Shenderova et al., 2007; Wu et al., 2015) and antibacterial abilities (Chatterjee et al., 2015; Wehling et al., 2014) of ND has been reported. ND could attenuate UV radiation through absorption and scattering, a phenomenon dependent on factors such as the ND particle size and nitrogen defects (Shenderova et al., 2007). ND as an energy absorber is applicable to sunscreen and a protective agent for photo-sensitive drugs. Wu et al. studied the UVB-blocking efficiencies of ND; ND showed 94% UVB-blocking efficiency at a nanomaterial concentration of 2 mg/cm^2 and protected keratinocytes, fibroblasts, and C57BL/6J mouse skin from UVB-induced inflammation (Wu et al., 2015). In addition, ND inhibited the growth of gram-negative bacteria via attachment to the bacterial cell wall (Chatterjee et al., 2015). Oxidized ND showed strong bactericidal activity in not only gram-negative bacteria, but also gram-positive (Wehling et al., 2014). The bactericidal activity of ND could be applicable in preservatives and improve the shelf-life of pharmaceuticals. ND can be functionalized in many ways due to its large, accessible, and tailorable external surface (Mochalin and Gogotsi, 2015). The functionalization of ND enables sophisticated surface functionalization without hindering the useful properties of the ND core. ND could improve not only physical properties (Mochalin et al., 2011; Sundar et al., 2014), but also various interesting properties leading to uses such as targeted drug delivery (Bertrand et al., 2015), sustained drug release (Cui et al., 2016), fluorescence (Bumb et al., 2013; Maitra et al., 2011), antioxidant (Adach et al., 2015), and pH-mediated drug delivery (Shimkunas et al., 2009; Zhao et al., 2014b).

Though injection formulation was the primarily researched drug delivery system, various formulations using ND has been sought. ND increased the photo-stability of eugenol and improved the *in vitro* skin permeation of eugenol by maintaining a high drug concentration through drug adsorption (Lim et al., 2016); this property is applicable for topical drug delivery. An ND-embedded nanogel showed a sustained release of glaucoma drugs from the hydrogel lens and proved the possibility of using NDs as an effective vehicle for the ocular delivery of bioactive molecules (Kim et al., 2014). A ND-conjugated scaffold showed induced bone formation in both *in vitro* and *in vivo* experiments (Suliman et al., 2015). NDs provide enhanced mechanical properties and a large surface area, which are favorable for implanted devices. The extended uses of ND as exogenous material are the main concerns of real applications in pharmaceuticals, together with the accurate understanding between the ND and drugs.

Overall, regarding newly emerging exogenous materials, ND was introduced as a drug delivery platform and its other biomedical applications were summarized in this review. Mainly by using the tools of physical adsorption and surface modification, the studies were extensively applied for diverse objectives. Together with the investigation of new applications, there are avenues of research to be examined for pharmaceutical formulation and the optimal design of the drug delivery systems, including targeting, smart activity, and organ-specific delivery. As ND is known for their inertness and their physical adsorption capability, their energy absorbance may also impact their employment in biomedical engineering and pharmaceutical applications.

Acknowledgment

This research was supported by the Bio & Medical Technology Development Program of the NRF funded by the Korean government, MSIP (NRF-2014M3A9A9073811) and the Basic Science Research Program through the National Research Foundation of Korea (NRF) funded by the Ministry of Science, ICT & Future Planning (NRF-2015R1C1A2A01053307).

References

Adach, K., Fijalkowski, M., Skolimowski, J., 2015. Antioxidant effect of hydroxylated diamond nanoparticles measured in soybean oil. Fuller. Nanotub. Carbon Nanostruct. 23, 1024–1032.
Adnan, A., Lam, R., Chen, H., Lee, J., Schaffer, D.J., Barnard, A.S., Schatz, G.C., Ho, D., Liu, W.K., 2011. Atomistic simulation and measurement of pH dependent cancer therapeutic interactions with nanodiamond carrier. Mol. Pharm. 8, 368–374.
Alhaddad, A., Adam, M.P., Botsoa, J., Dantelle, G., Perruchas, S., Gacoin, T., Mansuy, C., Lavielle, S., Malvy, C., Treussart, F., Bertrand, J.R., 2011. Nanodiamond as a vector for siRNA delivery to Ewing sarcoma cells. Small 7, 3087–3095.
Aramesh, M., Shimoni, O., Ostrikov, K., Prawer, S., Cervenka, J., 2015. Surface charge effects in protein adsorption on nanodiamonds. Nanoscale 7, 5726–5736.
Bacakova, L., Kopova, I., Stankova, L., Liskova, J., Vacik, J., Lavrentiev, V., Kromka, A., Potocky, S., Stranska, D., 2014. Bone cells in cultures on nanocarbon-based materials for potential bone tissue engineering: a review. Phys. Status Solidi A 211, 2688–2702.
Barnard, A.S., Per, M.C., 2014. Size and shape dependent deprotonation potential and proton affinity of nanodiamond. Nanotechnology 25, 445702.
Barnard, A.S., Sternberg, M., 2005. Substitutional nitrogen in nanodiamond and bucky-diamond particles. J. Phys. Chem. B 109, 17107–17112.
Barras, A., Lyskawa, J., Szunerits, S., Woisel, P., Boukherroub, R., 2011. Direct functionalization of nanodiamond particles using dopamine derivatives. Langmuir 27, 12451–12457.
Bertrand, J.-R., Pioche-Durieu, C., Ayala, J., Petit, T., Girard, H.A., Malvy, C.P., Le Cam, E., Treussart, F., Arnault, J.-C., 2015. Plasma hydrogenated cationic detonation nanodiamonds efficiently deliver to human cells in culture functional siRNA targeting the Ewing sarcoma junction oncogene. Biomaterials 45, 93–98.
Boudou, J.-P., Curmi, P.A., Jelezko, F., Wrachtrup, J., Aubert, P., Sennour, M., Balasubramanian, G., Reuter, R., Thorel, A., Gaffet, E., 2009. High yield fabrication of fluorescent nanodiamonds. Nanotechnology 20, 235602.
Bradac, C., Gaebel, T., Naidoo, N., Sellars, M.J., Twamley, J., Brown, L.J., Barnard, A.S., Plakhotnik, T., Zvyagin, A.V., Rabeau, J.R., 2010. Observation and control of blinking nitrogen-vacancy centres in discrete nanodiamonds. Nat. Nanotechnol. 5, 345–349.
Branson, B.T., Beauchamp, P.S., Beam, J.C., Lukehart, C.M., Davidson, J.L., 2013. Nanodiamond nanofluids for enhanced thermal conductivity. ACS Nano 7, 3183–3189.
Bumb, A., Sarkar, S.K., Billington, N., Brechbiel, M.W., Neuman, K.C., 2013. Silica encapsulation of fluorescent nanodiamonds for colloidal stability and facile surface functionalization. J. Am. Chem. Soc. 135, 7815–7818.
Cao, M., Deng, X., Su, S., Zhang, F., Xiao, X., Hu, Q., Fu, Y., Yang, B.B., Wu, Y., Sheng, W., Zeng, Y., 2013. Protamine sulfate-nanodiamond hybrid nanoparticles as a vector for MiR-203 restoration in esophageal carcinoma cells. Nanoscale 5, 12120–12125.
Chang, I.P., Hwang, K.C., Chiang, C.-S., 2008. Preparation of fluorescent magnetic nanodiamonds and cellular imaging. J. Am. Chem. Soc. 130, 15476–15481.
Chang, L.-Y., Ōsawa, E., Barnard, A.S., 2011. Confirmation of the electrostatic self-assembly of nanodiamonds. Nanoscale 3, 958–962.

Chatterjee, A., Perevedentseva, E., Jani, M., Cheng, C.-Y., Ye, Y.-S., Chung, P.-H., Cheng, C.-L., 2015. Antibacterial effect of ultrafine nanodiamond against gram-negative bacteria Escherichia coli. J. Biomed. Opt. 20 051014–051014.
Chen, M., Pierstorff, E.D., Lam, R., Li, S.Y., Huang, H., Osawa, E., Ho, D., 2009. Nanodiamond-mediated delivery of water-insoluble therapeutics. ACS Nano 3, 2016–2022.
Chernysheva, M.G., Myasnikov, I.Y., Badun, G.A., 2015. Myramistin adsorption on detonation nanodiamonds in the development of drug delivery platforms. Diam. Relat. Mater. 55, 45–51.
Chow, E.K., Zhang, X.-Q., Chen, M., Lam, R., Robinson, E., Huang, H., Schaffer, D., Osawa, E., Goga, A., Ho, D., 2011. Nanodiamond therapeutic delivery agents mediate enhanced chemoresistant tumor treatment. Sci. Transl. Med. 3 73ra21–73ra21.
Chu, H.L., Chen, H.W., Tseng, S.H., Hsu, M.H., Ho, L.P., Chou, F.H., Li, M., Chang, Y.C., Chen, P.H., Tsai, L.Y., 2014. Development of a growth-Hormone-Conjugated nanodiamond complex for cancer therapy. ChemMedChem 9, 1023–1029.
Cui, Z., Zhang, Y., Zhang, J., Kong, H., Tang, X., Pan, L., Xia, K., Aldalbahi, A., Li, A., Tai, R., 2016. Sodium alginate-functionalized nanodiamonds as sustained chemotherapeutic drug-release vectors. Carbon 97, 78–86.
Daulton, T., Kirk, M., Lewis, R., Rehn, L., 2001. Production of nanodiamonds by high-energy ion irradiation of graphite at room temperature. Nucl. Instrum. Meth. B 175, 12–20.
Faklaris, O., Joshi, V., Irinopoulou, T., Tauc, P., Sennour, M., Girard, H., Gesset, C., Arnault, J.C., Thorel, A., Boudou, J.P., Curmi, P.A., Treussart, F., 2009. Photoluminescent diamond nanoparticles for cell labeling: study of the uptake mechanism in mammalian cells. ACS Nano 3, 3955–3962.
Gaebel, T., Bradac, C., Chen, J., Say, J., Brown, L., Hemmer, P., Rabeau, J., 2012. Size-reduction of nanodiamonds via air oxidation. Diam. Relat. Mater 21, 28–32.
Guan, B., Zou, F., Zhi, J., 2010. Nanodiamond as the pH-responsive vehicle for an anticancer drug. Small 6, 1514–1519.
Havlik, J., Petrakova, V., Rehor, I., Petrak, V., Gulka, M., Stursa, J., Kucka, J., Ralis, J., Rendler, T., Lee, S.Y., Reuter, R., Wrachtrup, J., Ledvina, M., Nesladek, M., Cigler, P., 2013. Boosting nanodiamond fluorescence: towards development of brighter probes. Nanoscale 5, 3208–3211.
Hens, S.C., Cunningham, G., Tyler, T., Moseenkov, S., Kuznetsov, V., Shenderova, O., 2008. Nanodiamond bioconjugate probes and their collection by electrophoresis. Diam. Relat. Mater. 17, 1858–1866.
Hsieh, Y.H., Liu, K.K., Sulake, R.S., Chao, J.I., Chen, C., 2015. Microwave-assisted efficient conjugation of nanodiamond and paclitaxel. Bioorg. Med. Chem. Lett 25, 2074–2077.
Huang, H., Pierstorff, E., Osawa, E., Ho, D., 2007. Active nanodiamond hydrogels for chemotherapeutic delivery. Nano Lett. 7, 3305–3314.
Huang, H., Pierstorff, E., Osawa, E., Ho, D., 2008. Protein-mediated assembly of nanodiamond hydrogels into a biocompatible and biofunctional multilayer nanofilm. ACS Nano 2, 203–212.
Kim, H., Man, H.B., Saha, B., Kopacz, A.M., Lee, O.S., Schatz, G.C., Ho, D., Liu, W.K., 2012. Multiscale simulation as a framework for the enhanced design of nanodiamond-polyethylenimine-based gene delivery. J. Phys. Chem. Lett. 3, 3791–3797.
Kim, H.J., Zhang, K., Moore, L., Ho, D., 2014. Diamond nanogel-embedded contact lenses mediate lysozyme-dependent therapeutic release. ACS Nano 8, 2998–3005.
Kloss, F.R., Gassner, R., Preiner, J., Ebner, A., Larsson, K., Hächl, O., Tuli, T., Rasse, M., Moser, D., Laimer, K., 2008. The role of oxygen termination of nanocrystalline diamond on immobilisation of BMP-2 and subsequent bone formation. Biomaterials 29, 2433–2442.
Knapinska, A.M., Tokmina-Roszyk, D., Amar, S., Tokmina-Roszyk, M., Mochalin, V.N., Gogotsi, Y., Cosme, P., Terentis, A.C., Fields, G.B., 2015. Solid-phase synthesis characterization, and cellular activities of collagen-model nanodiamond-peptide conjugates. Peptide Sci. 104, 186–195.
Krueger, A., Lang, D., 2012. Functionality is key: recent progress in the surface modification of nanodiamond. Adv. Funct. Mater 22, 890–906.
Krueger, A., Stegk, J., Liang, Y., Lu, L., Jarre, G., 2008. Biotinylated nanodiamond: simple and efficient functionalization of detonation diamond. Langmuir 24, 4200–4204.
Krueger, A., 2008. New carbon materials: biological applications of functionalized nanodiamond materials. Chem.-Eur. J. 14, 1382–1390.
Kulakova, I., 2004. Surface chemistry of nanodiamonds. Phys. Status Solidi A 46, 636–643.
Kurantowicz, N., Strojny, B., Sawosz, E., Jaworski, S., Kutwin, M., Grodzik, M., Wierzbicki, M., Lipińska, L., Mitura, K., Chwalibog, A., 2015. Biodistribution of a high dose of diamond, graphite, and graphene oxide nanoparticles after multiple intraperitoneal injections in rats. Nanoscale Res. Lett. 10, 1–14.
Kuznetsov, O., Sun, Y., Thaner, R., Bratt, A., Shenoy, V., Wong, M.S., Jones, J., Billups, W.E., 2012. Water-soluble nanodiamond. Langmuir 28, 5243–5248.
Lai, L., Barnard, A.S., 2012. Nanodiamond for hydrogen storage: temperature-dependent hydrogenation and charge-induced dehydrogenation. Nanoscale 4, 1130–1137.
Lai, L., Barnard, A.S., 2014. Anisotropic adsorption and distribution of immobilized carboxyl on nanodiamond. Nanoscale 6, 14185–14189.
Lee, J.W., Lee, S., Jang, S., Han, K.Y., Kim, Y., Hyun, J., Kim, S.K., Lee, Y., 2013. Preparation of non-aggregated fluorescent nanodiamonds (FNDs) by non-covalent coating with a block copolymer and proteins for enhancement of intracellular uptake. Mol. Biosyst. 9, 1004–1011.
Lee, D.-K., Kim, S.V., Limansubroto, A.N., Yen, A., Soundia, A., Wang, C.-Y., Shi, W., Hong, C., Tetradis, S., Kim, Y., 2015. Nanodiamond–Gutta Percha composite biomaterials for root canal therapy. ACS Nano 9, 11490–11501.
Li, H.C., Hsieh, F.J., Chen, C.P., Chang, M.Y., Hsieh, P.C., Chen, C.C., Hung, S.U., Wu, C.C., Chang, H.C., 2013. The hemocompatibility of oxidized diamond nanocrystals for biomedical applications. Sci. Rep. 3, 3044.
Lien, Z.-Y., Hsu, T.-C., Liu, K.-K., Liao, W.-S., Hwang, K.-C., Chao, J.-I., 2012. Cancer cell labeling and tracking using fluorescent and magnetic nanodiamond. Biomaterials 33, 6172–6185.
Lim, C.H., Sorkin, A., Bao, Q., Li, A., Zhang, K., Nesladek, M., Loh, K.P., 2013. A hydrothermal anvil made of graphene nanobubbles on diamond. Nat. Commun. 4, 1556.
Lim, D.G., Kim, K.H., Kang, E., Lim, S.H., Ricci, J., Sung, S.K., Kwon, M.T., Jeong, S.H., 2016. Comprehensive evaluation of carboxylated nanodiamond as a topical drug delivery system. Int. J. Nanomed. 11, 2381–2395.
Lin, C.L., Lin, C.H., Chang, H.C., Su, M.C., 2015. Protein attachment on nanodiamonds. J. Phys. Chem. A 119, 7704–7711.
Liu, H., Dandy, D.S., 1995. Studies on nucleation process in diamond CVD: an overview of recent developments. Diam. Relat. Mater. 4, 1173–1188.
Liu, Y., Gu, Z., Margrave, J.L., Khabashesku, V.N., 2004. Functionalization of nanoscale diamond powder: fluoro- alkyl-, amino-, and amino acid-nanodiamond derivatives. Chem. Mater. 16, 3924–3930.
Liu, K.K., Wang, C.C., Cheng, C.L., Chao, J.I., 2009. Endocytic carboxylated nanodiamond for the labeling and tracking of cell division and differentiation in cancer and stem cells. Biomaterials 30, 4249–4259.
Liu, K.-K., Zheng, W.-W., Wang, C.-C., Chiu, Y.-C., Cheng, C.-L., Lo, Y.-S., Chen, C., Chao, J.-I., 2010. Covalent linkage of nanodiamond-paclitaxel for drug delivery and cancer therapy. Nanotechnology 21, 315106.
Maitra, U., Jain, A., George, S.J., Rao, C.N., 2011. Tunable fluorescence in chromophore-functionalized nanodiamond induced by energy transfer. Nanoscale 3, 3192–3197.
Man, H.B., Kim, H., Kim, H.J., Robinson, E., Liu, W.K., Chow, E.K., Ho, D., 2014. Synthesis of nanodiamond-daunorubicin conjugates to overcome multidrug chemoresistance in leukemia. Nanomed.-Nanotechnol 10, 359–369.
Mansoorianfar, M., Shokrgozar, M.A., Mehrjoo, M., Tamjid, E., Simchi, A., 2013. Nanodiamonds for surface engineering of orthopedic implants: enhanced biocompatibility in human osteosarcoma cell culture. Diam. Relat. Mater. 40, 107–114.
Manus, L.M., Mastarone, D.J., Waters, E.A., Zhang, X.-Q., Schultz-Sikma, E.A., MacRenaris, K.W., Ho, D., Meade, T.J., 2009. Gd(III)-nanodiamond conjugates for MRI contrast enhancement. Nano Lett. 10, 484–489.
Marcon, L., Riquet, F., Vicogne, D., Szunerits, S., Bodart, J.F., Boukherroub, R., 2010. Cellular and in vivo toxicity of functionalized nanodiamond in Xenopus embryos. J. Mater. Chem. 20, 8064–8069.
Mochalin, V.N., Gogotsi, Y., 2009. Wet chemistry route to hydrophobic blue fluorescent nanodiamond. J. Am. Chem. Soc. 131, 4594–4595.
Mochalin, V.N., Gogotsi, Y., 2015. Nanodiamond–polymer composites. Diam. Relat. Mater. 58, 161–171.
Mochalin, V.N., Neitzel, I., Etzold, B.J., Peterson, A., Palmese, G., Gogotsi, Y., 2011. Covalent incorporation of aminated nanodiamond into an epoxy polymer network. ACS Nano 5, 7494–7502.
Mochalin, V.N., Shenderova, O., Ho, D., Gogotsi, Y., 2012. The properties and applications of nanodiamonds. Nat. Nanotechnol. 7, 11–23.
Mochalin, V.N., Pentecost, A., Li, X.M., Neitzel, I., Nelson, M., Wei, C., He, T., Guo, F., Gogotsi, Y., 2013. Adsorption of drugs on nanodiamond: toward development of a drug delivery platform. Mol. Pharm. 10, 3728–3735.
Moore, L., Gatica, M., Kim, H., Osawa, E., Ho, D., 2013. Multi-protein delivery by nanodiamonds promotes bone formation. J. Dent. Res. (0022034513504952).
Moore, L., Grobarova, V., Shen, H., Man, H.B., Micova, J., Ledvina, M., Stursa, J., Nesladek, M., Fiserova, A., Ho, D., 2014. Comprehensive interrogation of the cellular response to fluorescent, detonation and functionalized nanodiamonds. Nanoscale 6, 11712–11721.
Nagl, A., Hemelaar, S.R., Schirhagl, R., 2015. Improving surface and defect center chemistry of fluorescent nanodiamonds for imaging purposes-a review. Anal. Bioanal. Chem..
Niu, K.Y., Zheng, H.M., Li, Z.Q., Yang, J., Sun, J., Du, X.W., 2011. Laser dispersion of detonation nanodiamonds. Angew. Chem. Int. Ed. Engl. 50, 4099–4102.
Paci, J.T., Man, H.B., Saha, B., Ho, D., Schatz, G.C., 2013. Understanding the surfaces of nanodiamonds. J. Phys. Chem. C 117, 17256–17267.
Paget, V., Sergent, J., Grall, R., Altmeyer-Morel, S., Girard, H., Petit, T., Gesset, C., Mermoux, M., Bergonzo, P., Arnault, J., 2014. Carboxylated nanodiamonds are neither cytotoxic nor genotoxic on liver, kidney, intestine and lung human cell lines. Nanotoxicology 8, 46–56.
Pentecost, A., Gour, S., Mochalin, V., Knoke, I., Gogotsi, Y., 2010. Deaggregation of nanodiamond powders using salt- and sugar-assisted milling. ACS Appl. Mater. Interfaces 2, 3289–3294.
Prabhakar, N., Nareoja, T., von Haartman, E., Sen Karaman, D., Jiang, H., Koho, S., Dolenko, T.A., Hanninen, P.E., Vlasov, D.I., Ralchenko, V.G., Hosomi, S., Vlasov, I.I., Sahlgren, C., Rosenholm, J.M., 2013. Core-shell designs of photoluminescent nanodiamonds with porous silica coatings for bioimaging and drug delivery II: application. Nanoscale 5, 3713–3722.
Rojas, S., Gispert, J.D., Martin, R., Abad, S., Menchon, C., Pareto, D., Victor, V.M., Alvaro, M., Garcia, H., Herance, J.R., 2011. Biodistribution of amino-functionalized diamond nanoparticles. In vivo studies based on 18 F radionuclide emission. ACS Nano 5, 5552–5559.

Ryu, T.K., Lee, G.J., Rhee, C.K., Choi, S.W., 2015. Cellular uptake behavior of doxorubicin-conjugated nanodiamond clusters for efficient cancer therapy. Macromol. Biosci..
Sabirov, D.S., Ōsawa, E., 2015. Dipole polarizability of nanodiamonds and related structures. Diam. Relat. Mater. 55, 64–69.
Salaam, A.D., Hwang, P., McIntosh, R., Green, H.N., Jun, H.W., Dean, D., 2014a. Nanodiamond-DGEA peptide conjugates for enhanced delivery of doxorubicin to prostate cancer. Beilstein. J. Nanotechnol. 5, 937–945.
Salaam, A.D., Hwang, P.T., Poonawalla, A., Green, H.N., Jun, H.W., Dean, D., 2014b. Nanodiamonds enhance therapeutic efficacy of doxorubicin in treating metastatic hormone-refractory prostate cancer. Nanotechnology 25, 425103.
Schinkel, A.H., Jonker, J.W., 2003. Mammalian drug efflux transporters of the ATP binding cassette (ABC) family: an overview. Adv. Drug Deliver. Rev. 55, 3–29.
Schrand, A.M., Dai, L., Schlager, J.J., Hussain, S.M., Osawa, E., 2007a. Differential biocompatibility of carbon nanotubes and nanodiamonds. Diam. Relat. Mater. 16, 2118–2123.
Schrand, A.M., Huang, H., Carlson, C., Schlager, J.J., Osawa, E., Hussain, S.M., Dai, L., 2007b. Are diamond nanoparticles cytotoxic? J. Phys. Chem. B 111, 2–7.
Schrand, A.M., Lin, J.B., Hens, S.C., Hussain, S.M., 2011. Temporal and mechanistic tracking of cellular uptake dynamics with novel surface fluorophore-bound nanodiamonds. Nanoscale 3, 435–445.
Shenderova, O., Grichko, V., Hens, S., Walch, J., 2007. Detonation nanodiamonds as UV radiation filter. Diam. Relat. Mater. 16, 2003–2008.
Shimkunas, R.A., Robinson, E., Lam, R., Lu, S., Xu, X., Zhang, X.Q., Huang, H., Osawa, E., Ho, D., 2009. Nanodiamond-insulin complexes as pH-dependent protein delivery vehicles. Biomaterials 30, 5720–5728.
Suliman, S., Xing, Z., Wu, X., Xue, Y., Pedersen, T.O., Sun, Y., Døskeland, A.P., Nickel, J., Waag, T., Lygre, H., 2015. Release and bioactivity of bone morphogenetic protein-2 are affected by scaffold binding techniques in vitro and in vivo. J. Control. Release 197, 148–157.
Sundar, L.S., Singh, M.K., Ramana, E.V., Singh, B., Gracio, J., Sousa, A.C., 2014. Enhanced thermal conductivity and viscosity of nanodiamond-nickel nanocomposite nanofluids. Sci. Rep. 4, 4039.
Toh, T.B., Lee, D.K., Hou, W., Abdullah, L.N., Nguyen, J., Ho, D., Chow, E.K., 2014. Nanodiamond-mitoxantrone complexes enhance drug retention in chemoresistant breast cancer cells. Mol. Pharm 11, 2683–2691.
Tsapikouni, T.S., Missirlis, Y.F., 2008. Protein–material interactions: from micro-to-nano scale. Mater. Sci. Eng. B-Adv. 152, 2–7.
Vaijayanthimala, V., Cheng, P.Y., Yeh, S.H., Liu, K.K., Hsiao, C.H., Chao, J.I., Chang, H.C., 2012. The long-term stability and biocompatibility of fluorescent nanodiamond as an in vivo contrast agent. Biomaterials 33, 7794–7802.
Wahab, Z., Foley, E.A., Pellechia, P.J., Anneaux, B.L., Ploehn, H.J., 2015. Surface functionalization of nanodiamond with phenylphosphonate. J. Coll. Interf. Sci. 450, 301–309.
Wang, H.D., Yang, Q.Q., Niu, C.H., Badea, I., 2012. Adsorption of azo dye onto nanodiamond surface. Diam. Relat. Mater. 26, 1–6.
Wang, D., Tong, Y., Li, Y., Tian, Z., Cao, R., Yang, B., 2013. PEGylated nanodiamond for chemotherapeutic drug delivery. Diam. Relat. Mater. 36, 26–34.
Wang, X., Low, X.C., Hou, W., Abdullah, L.N., Toh, T.B., Mohd Abdul Rashid, M., Ho, D., Chow, E.K., 2014. Epirubicin-adsorbed nanodiamonds kill chemoresistant hepatic cancer stem cells. ACS Nano 8, 12151–12166.
Wang, Z., Tian, Z., Dong, Y., Li, L., Tian, L., Li, Y., Yang, B., 2015. Nanodiamond-conjugated transferrin as chemotherapeutic drug delivery. Diam. Relat. Mater 58, 84–93.
Wehling, J., Dringen, R., Zare, R.N., Maas, M., Rezwan, K., 2014. Bactericidal activity of partially oxidized nanodiamonds. ACS Nano 8, 6475–6483.
Wrachtrup, J., 2010. Nanoparticles: switching blinking on and off. Nat. Nanotechnol. 5, 314–315.
Wu, M.-S., Sun, D.-S., Lin, Y.-C., Cheng, C.-L., Hung, S.-C., Chen, P.-K., Yang, J.-H., Chang, H.-H., 2015. Nanodiamonds protect skin from ultraviolet B-induced damage in mice. J. Nanobiotechnol. 13, 35.
Xiao, J., Duan, X., Yin, Q., Zhang, Z., Yu, H., Li, Y., 2013. Nanodiamonds-mediated doxorubicin nuclear delivery to inhibit lung metastasis of breast cancer. Biomaterials 34, 9648–9656.
Xing, Y., Xiong, W., Zhu, L., Osawa, E., Hussin, S., Dai, L.M., 2011. DNA damage in embryonic stem cells caused by nanodiamonds. ACS Nano 5, 2376–2384.
Xing, Z., Pedersen, T.O., Wu, X., Xue, Y., Sun, Y., Finne-Wistrand, A., Kloss, F.R., Waag, T., Krueger, A., Steinmüller-Nethl, D., 2013. Biological effects of functionalizing copolymer scaffolds with nanodiamond particles. Tissue Eng. Pt, A 19, 1783–1791.
Xu, Q., Zhao, X., 2012. Electrostatic interactions versus van der Waals interactions in the self-assembly of dispersed nanodiamonds. J. Mater. Chem. 22, 16416–16421.
Xu, X.Y., Zhu, Y.W., Wang, B.C., Yu, Z.M., Xie, S.Z., 2005. Mechanochemical dispersion of nanodiamond aggregates in aqueous media\. J. Mater. Sci. Technol. 21, 109–112.
Zeng, X., Morgenstern, R., Nyström, A.M., 2014. Nanoparticle-directed sub-cellular localization of doxorubicin and the sensitization breast cancer cells by circumventing GST-mediated drug resistance. Biomaterials 35, 1227–1239.
Zhang, X.-Q., Chen, M., Lam, R., Xu, X., Osawa, E., Ho, D., 2009. Polymer-functionalized nanodiamond platforms as vehicles for gene delivery. ACS Nano 3, 2609–2616.
Zhang, Z., Niu, B., Chen, J., He, X., Bao, X., Zhu, J., Yu, H., Li, Y., 2014. The use of lipid-coated nanodiamond to improve bioavailability and efficacy of sorafenib in resisting metastasis of gastric cancer. Biomaterials 35, 4565–4572.
Zhao, L., Xu, Y.H., Akasaka, T., Abe, S., Komatsu, N., Watari, F., Chen, X., 2014a. Polyglycerol-coated nanodiamond as a macrophage-evading platform for selective drug delivery in cancer cells. Biomaterials 35, 5393–5406.
Zhao, L., Xu, Y.H., Qin, H., Abe, S., Akasaka, T., Chano, T., Watari, F., Kimura, T., Komatsu, N., Chen, X., 2014b. Platinum on nanodiamond: a promising prodrug conjugated with stealth polyglycerol: targeting peptide and acid-responsive antitumor drug. Adv. Funct. Mater. 24, 5348–5357.
Zhu, Y., Li, J., Li, W., Zhang, Y., Yang, X., Chen, N., Sun, Y., Zhao, Y., Fan, C., Huang, Q., 2012. The biocompatibility of nanodiamonds and their application in drug delivery systems. Theranostics 2, 302–312.